International Journal of Nanomedicine

Dovepress
open access to scientific and medical research

Open Access Full Text Article

ORIGINAL RESEARCH

Exosomal miR-133a-3p Derived from BMSCs Alleviates Cerebral Ischemia-Reperfusion Injury via Targeting DAPK2

Xuanyong Yang[1,*], Jiang Xu[1,*], Shihai Lan[1], Zhigao Tong[1], Kang Chen[1], Zhizheng Liu[1], Shan Xu[2]

[1]Department of Neurosurgery, The First Affiliated Hospital, Nanchang University, Nanchang, People's Republic of China; [2]Department of Pathology, The First Affiliated Hospital of Nanchang University, Nanchang, People's Republic of China

*These authors contributed equally to this work

Correspondence: Shan Xu, Department of Pathology, The First Affiliated Hospital of Nanchang University, No. 17 Yong Wai Street, Nanchang, Jiangxi, 330006, People's Republic of China, Email xshan2002@126.com

Background: Cerebral ischemia-reperfusion (CI/R) injury is a subtype of complication after treatment of ischemic stroke. It has been reported that exosomes derived from BMSCs could play an important role in CI/R injury. However, whether BMSCs-derived exosomes could regulate CI/R injury via carrying miRNAs remains to be further explored.

Methods: RNA sequencing was performed to identify the differentially expressed miRNAs. To mimic CI/R in vitro, SH-SY5Y cells were exposed to oxygen glucose deprivation/reoxygenation (OGD/R). The viability of SH-SY5Y cells was tested by CCK8 assay, and TUNEL staining was performed to detect the cell apoptosis.

Results: MiR-133a-3p was identified to be reduced in exosomes derived from the plasma of patients with IS. Upregulation of miR-133a-3p significantly reversed OGD/R-induced SH-SY5Y cell growth inhibition. Consistently, BMSCs-derived exosomal miR-133a-3p could restore OGD/R-decreased SH-SY5Y cell proliferation via inhibiting apoptosis. Meanwhile, DAPK2 was a direct target of miR-133a-3p. In addition, OGD/R notably upregulated the level of DAPK2 and weakened the expressions of p-Akt and p-mTOR in SH-SY5Y cells, whereas exosomal miR-133a-3p derived from BMSCs notably reversed these phenomena. Exosomal miR-133a-3p derived from BMSCs could reverse OGD/R-induced cell apoptosis via inhibiting autophagy. Furthermore, exosomal miR-133a-3p derived from BMSCs markedly alleviated the symptom of CI/R injury in vivo.

Conclusion: Exosomal miR-133a-3p derived from BMSCs alleviates CI/R injury via targeting DAPK2/Akt signaling. Thus, our study might shed new light on discovering new strategies against CI/R injury.

Keywords: CI/R, BMSC, miR-133a-3p, DAPK2, autophagy

Introduction

Ischemic stroke (IS) causes more than 40 million disabilities all over the world every year, and it often results in the disability among adults.[1] Nowadays, immediate restoration of the blood supply is the main strategy against IS, while it may cause the brain injury for sake of CI/R.[2] Indeed, the therapeutic effects of surgery and drug administration against CI/R remain not ideal. Therefore, it is essential to find novel strategies against CI/R injury.

It has been reported that the transplantation of bone marrow mesenchymal stem cells (BMSCs) was able to induce the nerve function recovery after cerebral ischemia.[3] Additionally, a recent study indicated that BMSCs could alleviate the progression of CI/R injury through mediation of PI3K/Akt/mTOR signaling pathway.[4] More importantly, recent studies demonstrated that BMSCs-derived exosomes (BMSC-exos) were able to act as crucial mediators in the biological function of BMSCs.[5,6] BMSC-secreted exosomes were able to influence the biological features of target cells via their interaction with the transfer of receptors between cells, specific ligand receptors and the transfer of RNAs and proteins.[7,8]

Received: 10 August 2022
Accepted: 3 December 2022
Published: 5 January 2023

Meanwhile, a previous study suggested that BMSC-derived exosomes were able to attenuate CI/R injury through modulation of autophagy.[5] Therefore, exosomes derived from BMSCs could play important roles in CI/R injury.

MicroRNAs (miRNAs), a subtype of non-coding RNAs, play vital roles in the development of CI/R.[9] Shi et al demonstrated that miR-532-5p inhibition could aggravate CI/R injury through negatively regulating CXCL1.[10] Upregulation of miR-652 ameliorated CI/R-induced neuron injury by mediation of NOX2.[11] Furthermore, BMSC-derived exosomes were able to modulate the process of multiple diseases via carrying miRNAs.[7,12] However, the function of exosomal miRNAs derived from BMSCs in CI/R injury remains further exploring.

Based on the above backgrounds, this study aimed to detect the differentially expressed miRNAs in exosomes derived from plasma of patients with IS. We hope this work would supply a novel method against CI/R injury.

Materials and Methods

Sample Collection

Plasma of patients with IS (n=20) and healthy people (n=20) were collected from the First Affiliated Hospital of Nanchang University between August 2020 and May 2021. The data of patients and healthy people were collected with their written informed consent. The samples were stored at −80°C and then used for RT-qPCR analysis and exosome isolation. The Ethics Committee of The First Affiliated Hospital of Nanchang University approved this study.

Cell Culture

SH-SY5Y cells were bought from ATCC (USA) and cultured with DMEM containing 10% FBS in the condition of 95% N_2/5% CO_2. For the purpose of constructing OGD model, PC12 cells (Chinese Academy of Sciences, Shanghai, China) were firstly cultured in medium without deoxygenated glucose. Subsequently, cells were incubated in condition of 95% N_2/5% CO_2 for 4 h (placed in a hypoxic vessel). Then, cells were transferred to DMEM containing 10% FBS and high glucose in condition of 95%/5% CO_2 for 24 h at 37°C.

Reagents

Rapamycin was obtained from Sigma (USA).

BMSC Isolation and Culture

BMSCs were obtained from mice (C57BL/6, 18–22 g) which were intraperitoneally administered with pentobarbital, and the femurs were removed. The femoral bone marrow cavity was washed, and the primary cells were maintained in DMEM (low-glucose) containing FBS (10%). The primary and third-generation BMSCs were used in subsequent analysis. The ethical committee of the First Affiliated Hospital of Nanchang University approved this study. Meanwhile, the isolated BMSCs were identified by microscopy and detection of CD90, CD29, CD34 and CD45 as previously described.[13,14]

Alizarin Red Staining Assay

The identification of third-generation BMSCs was assessed by alizarin red staining. Cells cultured in 12-well plates were rinsed with phosphate buffered saline (PBS) buffer (pH 7.4) for 3 times and fixed with 4% paraformaldehyde for 30 min. Afterwards, cells were stained with 1% alizarin red S solution (pH=8.4) (Sigma-Aldrich) for 5 min. Thereafter, cells were washed with PBS for 3 times and observed under a light microscope. The result was presented by photomicrographs of calcium nodules.

Oil Red O Staining

Oil Red O staining was used to identify the primary BMSCs. In brief, cells were fixed with 10% formalin at room temperature for 1 h and washed by 60% isopropanol. Then, 0.2% oil red O was used to stain the cells at room temperature for 10 min. Cells were then washed 3 times with ddH_2O. Excessive oil red O was removed by incubating cells with 1 mL isopropanol on a mild shaker for 10 min at room temperature. The images were observed under a microscope.

Exosome Isolation and Identification

BMSCs were centrifuged (15 min at 300 × g, 2000 × g for 15 min and 10,000 × g for 30 min) and then the supernatants were collected. Cell supernatants were used to extract exosomes using ultracentrifugation (70 min at 120,000 × g). NTA was performed to evaluate the particle sizes of exosomes, TEM was used to confirm the exosome structure and Western blot was used to identify the exosome markers.

RNA Sequencing

Total RNA was extracted from the exosomes derived from plasma of patients and healthy people by using TRIzol® (Takara, Tokyo, Japan) and then sent to GMINIX Co., Ltd. (Shanghai, China) for RNA sequencing.

Volcano plot and heatmap were performed to identify miRNA levels between exosomes from plasma of patients and healthy people, and R analysis was performed to evaluate the data.

Exosome Labeling and Uptake

SH-SY5Y cells were incubated with BMSCs-derived exosomes for 24 h. Cells were stained with PKH26 at 4°C overnight. Subsequently, fluorescent phalloidin was used to stain the cytoskeleton at 4°C. Then, DAPI was used to stain the nuclei for 5 min. Fluorescence microscope (magnification, x200; Olympus) was used to observe the result.

Cell Transfection

BMSCs and SH-SY5Y cells were transfected with miR-133a-3p mimics (Genepharma) or negative control (NC, Genepharma) by Lipofectamine 2000 in accordance with the protocol of manufacturer.

RT-qPCR

TRIzol (Takara) was used to isolate total RNA, and then PrimeScript RT (ELK bioscience) was used to reverse transcribe RNA into cDNA. Next, qPCR was performed using SYBR kit (ELK bioscience) on a 7900HT system. The primers used were as follows: for miR-133a-3p, 5'-AGGAACTGATTGGACTCAACTGAA-3' (forward) and 5'-CTCAACTGGTGTCGTGGAGTC-3'. (reverse); for DAPK2, 5'-ATTCCCAGTCAGAGGCGCTAT-3' (forward) and 5'-GAACTTGTCTTCCCGTCGTGT-3' (reverse); for β-actin: 5'-GTCCACCGCAAATGCTTCTA-3' (forward) and 5'-TGCTGTCACCTTCACCGTTC-3' (reverse) and for U6, 5'-CTCGCTTCGGCAGCACAT-3' (forward) and 5'-AACGCTTCACGAATTTGCGT-3' (reverse). β-Actin or U6 is the internal reference gene. The relative RNA levels were quantified using the $2^{-\Delta\Delta Ct}$ method.

CCK-8 Assay

SH-SY5Y cells (5.0×10^3) were treated with OGD/R, OGD/R + NC, OGD/R + miR-133a-3p mimics, OGD/R + BMSCs/NC-Exo or OGD/R + BMSCs/miR-133a-3p-Exo for 48 h. Afterwards, cells were exposed to 10 μL CCK-8 (Beyotime) for another 2 h at 37°C. The absorbance was assessed by microplate reader (Bio-Rad) at 450 nm.

Western Blot Assay

BCA kit (Beyotime) was used for protein quantification. Proteins were separated by 10% SDS-PAGE. Subsequently, proteins were blotted onto PVDF membranes. The primary antibodies: anti-CD63 (1:1000), anti-CD9 (1:1000), anti-CD81 (1:1000), anti-DAPK2 (1:1000), anti-Akt (1:1000), anti-p-Akt (1:1000), anti-mTOR (1:1000), anti-p-mTOR (1:1000), anti-Beclin 1 (1:1000) and anti-β-actin (1:1000) were used to incubate the membranes. Then, secondary antibody (HRP-conjugated; 1:5000) was used to incubate the membranes for 1 h. These antibodies were provided with Abcam. ECL kit was used for visualization of protein bands.

Elisa

The level of MDA, SOD, GSH-Px and LDH in SH-SY5Y cell supernatants were assessed by ELISA kit (ELK biotechnology) in line with the protocol of manufacturer.

Immunofluorescence

Cells were seeded in 24-well plates overnight. After treatment for 48 h, cells were blocked with 10% goat serum for 30 min at room temperature and then incubated with anti-EdU or anti-FJB antibody (Abcam, Cambridge, MA, USA; 1:1000) at 4°C overnight, followed by incubation with goat anti-rabbit IgG (Abcam; 1:5000) at 37°C for 1 h. Then, the nuclei were stained with DAPI (Beyotime, Shanghai, China) for 5 min. Finally, cells were observed under a fluorescence microscope (Olympus CX23, Tokyo, Japan).

Luciferase Reporter Assays

3'-UTR of DAPK2 containing the putative binding sites of miR-133a-3p was synthetized and obtained from Sangon Biotech (Shanghai, China), which were then cloned into the pmirGLO vector (Promega, Madison, WI, USA) to construct wild-type or mutate-type reporter vector DAPK2 (WT/MT). The DAPK2 (WT/MT) was transfected into cells together with control,

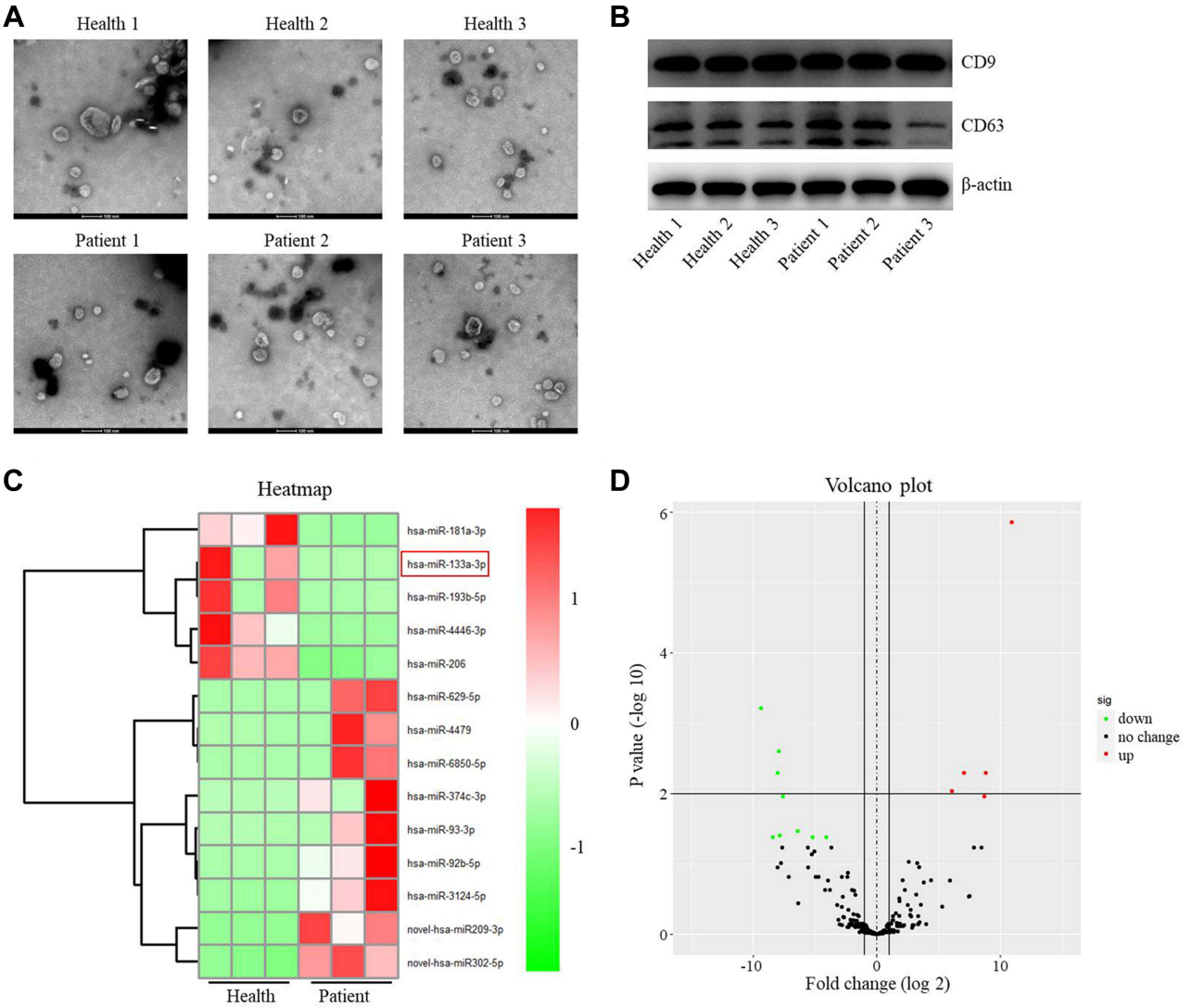

Figure 1 Differentially expressed miRNAs between exosomes derived from plasma of healthy people and patients with IS. (**A**) The extracellular vesicles were extracted from the plasma of patients with IS (n=3) or healthy people (n=3). Then, the extracellular vesicles were identified by TEM. (**B**) The expressions of CD9 and CD63 in extracellular vesicles from healthy people and patients with IS were detected by Western blot. (**C**) The differentially expressed miRNAs between the exosomes from healthy people and patients with IS were assessed using heatmap. (**D**) Volcano plots illustrating the differentially expressed miRNAs in IS. Red indicates a higher expression level, while green indicates a lower expression level.

vector-control (NC) or miR-133a-3p mimics using Lipofectamine 2000 (Thermo Fisher Scientific) according to the manufacturer's instructions. The relative luciferase activity was analyzed by the Dual-Glo Luciferase Assay System (Promega).

TUNEL Staining

Apoptosis was also determined by the TUNEL assay according to the manufacturer's instructions. Briefly, cells were fixed with 4% paraformaldehyde, and then incubated with 50 μL TUNEL reaction mixtures in a wet box for 60 min at 37°C in the dark. For signal conversion, cells were incubated with 50 μL of peroxidase (POD) for 30 min at 37°C, rinsed with PBS, and then incubated with 50 μL diaminobenzidine (DAB) substrate solution for 10 min at 25°C. Meanwhile, the nuclei was stained with DAPI for 5 min. Finally, the expression of apoptotic cells was observed under an optical microscope.

In vivo Experiment

Wistar rats (6-week-old) were bought from Vital River, and they were placed in a condition of specific pathogen-free facility. The rats were divided into sham (n=18), MCAO (n=18), MCAO + BMSCs/NC-Exos (n=18) and MCAO + BMSCs/miR-133a-3p-Exos (n=18) group. For establishment of in vivo model, rats were treated with 45 mg/kg sodium pentobarbital, and a surgical filament was used to occlude the middle cerebral artery (MCA) except sham group. After 1 h of MCA occlusion, the filament was removed, and reperfusion proceeded. Then, rats in sham and MCAO groups were administered with saline through intraventricular. Rats in other two groups were treated with BMSCs/NC-Exos or BMSCs/miR-133a-3p-Exos via the brain cavity. Finally, rats were sacrificed after 1 day or 7 days of MCAO treatment,

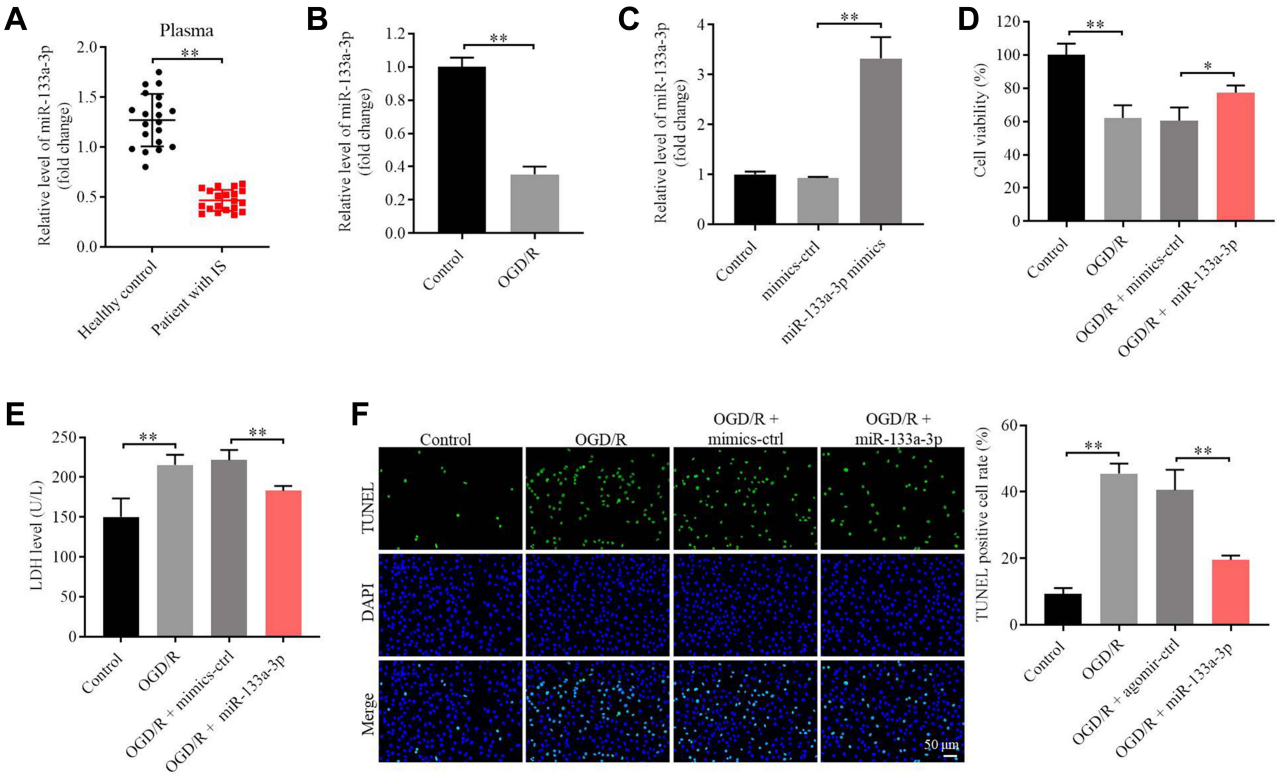

Figure 2 MiR-133a-3p upregulation reversed OGD/R-induced apoptosis in SH-SY5Y cells. (**A**) The expression of miR-133a-3p in plasma of healthy people or patients with IS was investigated by RT-qPCR. (**B**) SH-SY5Y cells were treated with OGD/R. The level of miR-133a-3p in SH-SY5Y cells was tested by RT-qPCR. (**C**) SH-SY5Y cells were transfected with NC or miR-133a-3p mimics. The expression of miR-133a-3p in SH-SY5Y cells was tested by RT-qPCR. (**D**) SH-SY5Y cells were treated with OGD/R, OGD/R + mimics-ctrl or OGD/R + miR-133a-3p mimics. The viability of SH-SY5Y cells was tested by CCK8 assay. (**E**) The LDH level in supernatants of SH-SY5Y cells was tested by ELISA. (**F**) The apoptosis in SH-SY5Y cells was tested by TUNEL staining. *P<0.05, **P< 0.01.

and the brain tissues were collected for the subsequent analysis. All experiments were performed in line with the NIH Guide, and Ethics Committees of The First Affiliated Hospital of Nanchang University approved this study. Meanwhile, neurological severity scores were evaluated, and Morris Water Maze analysis was performed as previously described.[15]

TTC Staining

The brain tissues were sliced into sections (2-mm-thick), and TTC (2%, Sigma) reagent was used to incubate the sections. Then, the sections were photographed using a digital camera. The cerebral infarction area was presented by calculating the percentage of total infarct volume/total brain volume × 100%.

Statistical Analysis

All experiments were repeated three times. Mean ± standard error (SD) was used to express the data. One-way analysis of variance (ANOVA) and post hoc Tukey's tests were used for comparisons between at least three groups. Values of $P<0.05$ indicated significant change.

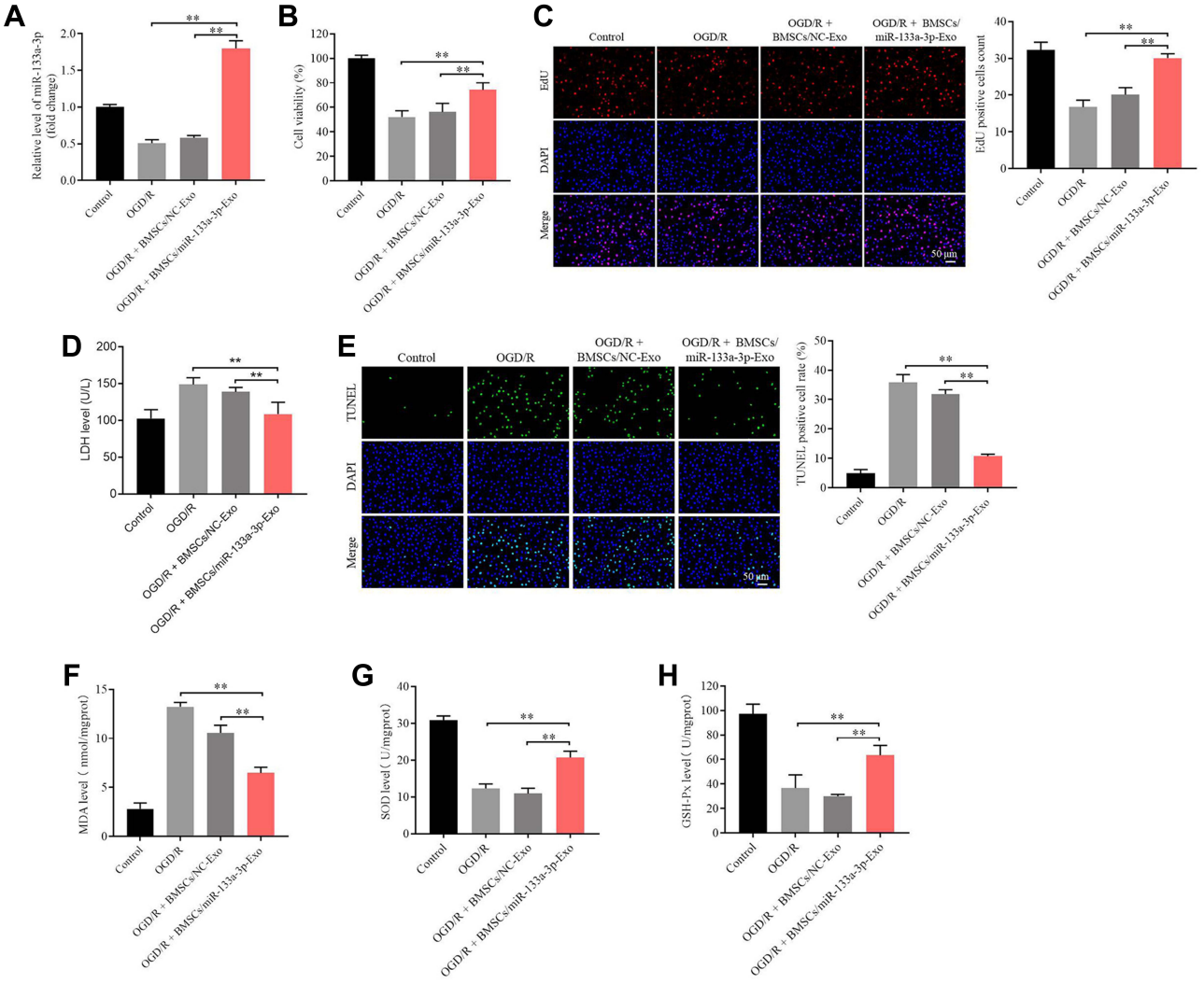

Figure 3 Exosomal miR-133a-3p derived from BMSCs reversed OGD/R-induced SH-SY5Y cell injury. SH-SY5Y cells were treated with OGD/R, OGD/R + BMSCs/NC-Exo or OGD/R + BMSCs/miR-133a-3p-Exo. (**A**) The level of miR-133a-3p in SH-SY5Y cells was investigated by RT-qPCR. (**B**) The viability of SH-SY5Y cells was tested by CCK8 assay. (**C**) The proliferation of SH-SY5Y cells was detected by EdU staining. (**D**) The LDH level in supernatants of SH-SY5Y cells was tested by ELISA. (**E**) The apoptosis in SH-SY5Y cells was tested by TUNEL staining. (**F**–**H**) The levels of MDA, SOD and GSH-Px in supernatants of SH-SY5Y cells were investigated by ELISA. **P< 0.01.

Results

Differentially Expressed miRNAs (DEmiRNAs) Between Exosomes Derived from Plasma of Healthy People and Patients with IS

Exosomes were isolated from the plasma of healthy people and patients with IS, and then identified by TEM. The typical rounded particles (30–150 nm in diameter) were observed (Figure 1A). In addition, CD9 and CD63 were highly

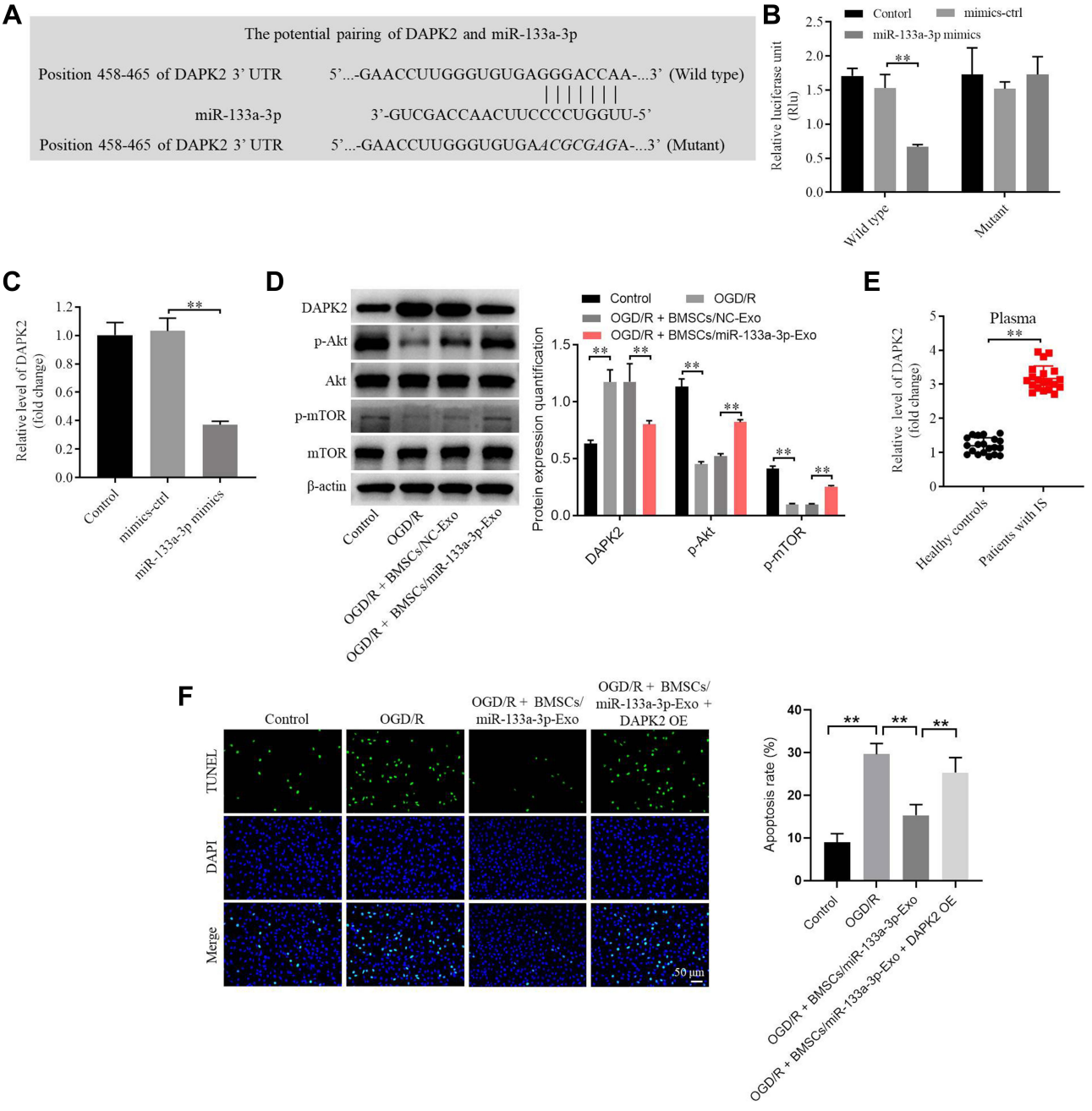

Figure 4 MiR-133a-3p directly targeted DAPK2. (**A**) Targetscan was used to predict the downstream mRNA of miR-133a-3p. (**B**) The relative luciferase activity in WT/MT-DAPK2 was detected by dual luciferase assay. (**C**) SH-SY5Y cells were transfected with mimics-ctrl or miR-133a-3p mimics. The levels of DAPK2 in SH-SY5Y cells were tested by RT-qPCR. (**D**) SH-SY5Y cells were treated with OGD/R, OGD/R + BMSCs/NC-Exo or OGD/R + BMSCs/miR-133a-3p-Exo. The protein levels of DAPK2, Akt, p-Akt, mTOR and p-mTOR in SH-SY5Y cells were investigated by Western blot. (**E**) The level of DAPK2 in plasma of patients with IS and healthy people was tested by RT-qPCR. (**F**) SH-SY5Y cells were treated with OGD/R, OGD/R + BMSCs/miR-133a-3p-Exo or OGD/R + BMSCs/miR-133a-3p-Exo + DAPK2 OE. The apoptosis of SH-SY5Y cells was tested by TUNEL staining. **P< 0.01.

expressed in these isolated vesicles (Figure 1B), suggesting exosomes were collected from plasma of healthy controls and patients with IS successfully.

To identify the DEmiRNAs between exosomes derived from plasma of healthy people and patients with IS, RNA sequencing was performed. The outcomes were presented with heatmap and volcano plot (Figure 1C and D). Among these DEmiRNAs, 5 were downregulated and 9 were upregulated in exosomes derived from plasma of patients with IS (Figure 1D). Meanwhile, miR-133a-3p was known to be involved in neuron injury,[16] and other differentially expressed miRNAs were pre-miRNAs. Thus, we focused on exploring the role of miR-133a-3p in CI/R.

MiR-133a-3p Upregulation Reversed OGD/R-Induced SH-SY5Y Cell Apoptosis

We next explored the role of miR-133a-3p in CI/R. As indicated in Figure 2A, the level of miR-133a-3p was notably lessened in plasma of patients with IS compared with that in healthy people. Consistently, miR-133a-3p level was significantly downregulated in SH-SY5Y cells exposed to OGD/R (Figure 2B). Additionally, miR-133a-3p level in SH-SY5Y cells was notably upregulated by miR-133a-3p mimics (Figure 2C). Moreover, OGD/R markedly inhibited SH-SY5Y cell viability, whereas miR-133a-3p upregulation reversed this phenomenon (Figure 2D). Meanwhile, the level of LDH in SH-SY5Y cell supernatants was significantly increased by OGD/R, which was partly overturned by miR-133a-3p overexpression (Figure 2E). Furthermore, OGD/R notably induced the apoptosis in SH-SY5Y cells, while the phenomenon was abolished by upregulation of miR-133a-3p (Figure 2F). Taken together, miR-133a-3p upregulation could suppress the apoptosis in SH-SY5Y cells exposed to OGD/R.

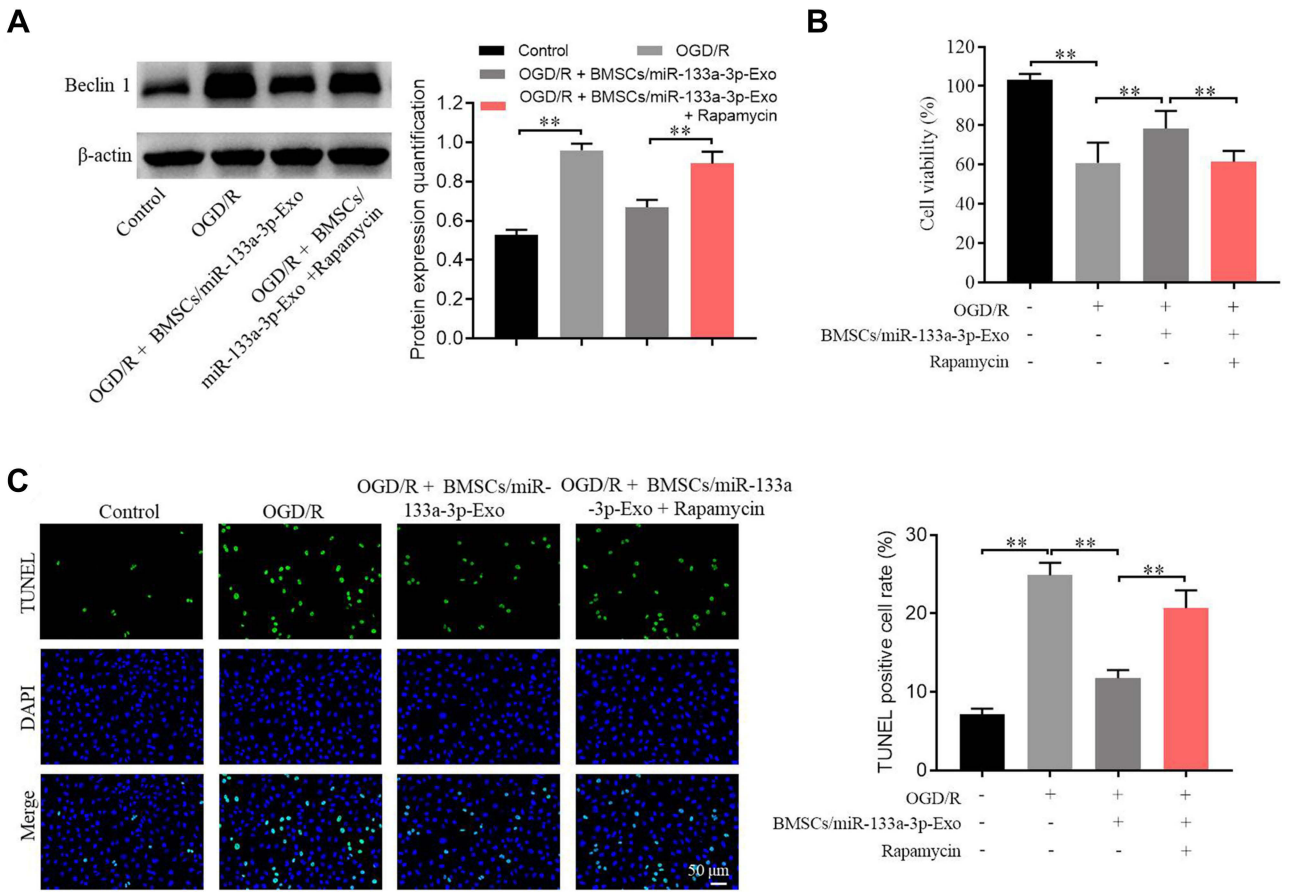

Figure 5 Exosomal miR-133a-3p derived from BMSCs alleviated OGD/R-induced SH-SY5Y cell apoptosis via inhibiting the autophagy. SH-SY5Y cells were treated with OGD/R, OGD/R + BMSCs/miR-133a-3p-Exo or OGD/R + BMSCs/miR-133a-3p-Exo + Rapamycin. (**A**) The protein level of Beclin-1 in SH-SY5Y cells was tested by Western blot. (**B**) The viability of SH-SY5Y cells was tested by CCK8 assay. (**C**) The apoptosis of SH-SY5Y cells was tested by TUNEL staining. **P< 0.01.

BMSCs Were Successfully Isolated from Mice

It has been reported that BMSCs were able to regulate the progression of CI/R injury.[6] Thus, BMSCs were isolated from mice and then the efficiency of cell isolation was identified. The data revealed that CD90 and CD29 were highly expressed, while CD34 and CD45 were lowly expressed in cells (CD90, CD29, CD34 and CD45 were key markers of third-generation BMSCs) (Supplementary Figure 1A and B). In addition, primary BMSCs exerted adipogenic differentiation, while third-generation BMSCs exhibited osteogenic differentiation (Supplementary Figure 1C). In summary, BMSCs were successfully isolated from mice, and third-generation BMSCs were selected in subsequent analysis.

MiR-133a-3p Can Be Transferred from BMSCs to SH-SY5Y Cells via Exosomes

BMSCs-derived exosomes were known to act as important mediators in CI/R injury.[5] Thus, exosomes were isolated from BMSCs, and the isolated extracellular vesicles were identified by NTA. The data showed that the size distribution was similar to the exosomes (Supplementary Figure 2A). In addition, the vesicles were rounded particles (30–150 nm in diameter) (Supplementary Figure 2B). CD9 and CD81 were highly expressed in extracellular vesicles from BMSCs (BMSCs-Exo, BMSCs/NC-Exo or BMSCs/miR-133a-3p-Exo) (Supplementary Figure 2C). To investigate the function of exosomes in the crosstalk between BMSCs and SH-SY5Y cells, SH-SY5Y cells were incubated with BMSCs-derived

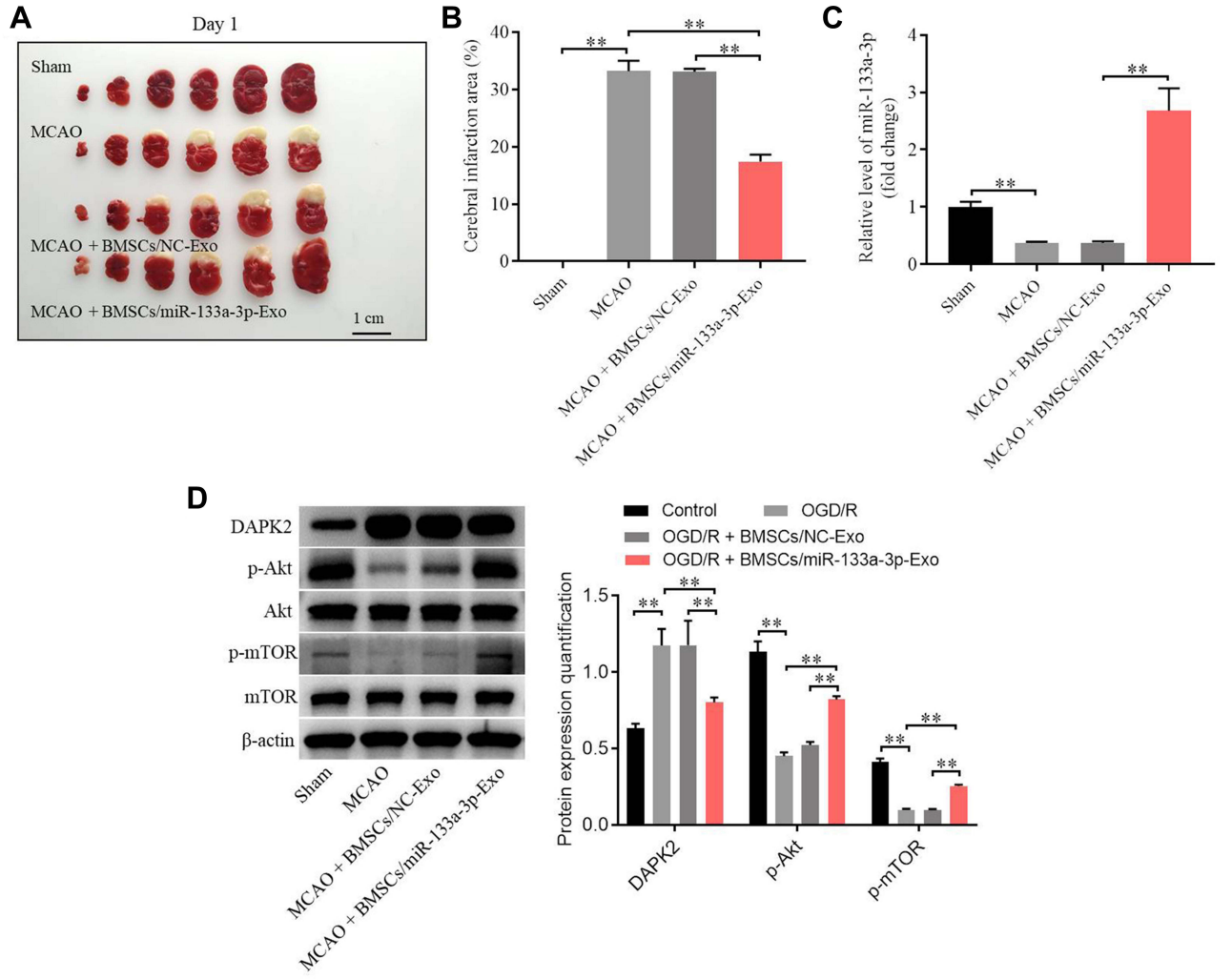

Figure 6 Exosomal miR-133a-3p derived from BMSCs markedly attenuated the symptom of CI/R injury in vivo. In vivo middle cerebral artery occlusion (MCAO) model in rats was established. At the end of the study, rats were sacrificed and the brain tissues were collected. Then, (**A**) the brain tissues were pictured, and TTC staining was performed to observe the severity of CI/R injury. (**B**) Cerebral infarction area was detected. (**C**) The expression of miR-133a-3p in tissues of rats was detected by RT-qPCR. (**D**) The protein levels of DAPK2, Akt, p-Akt, mTOR and p-mTOR in SH-SY5Y cells were investigated by Western blot. **P< 0.01.

PKH26-labeled exosomes. After incubation for 48 h, PKH26 lipid dye could be found in SH-SY5Y cells, and this result indicated that BMSCs-Exo could be transferred to SH-SY5Y cells (Supplementary Figure 2D). Meanwhile, RNase-A did not affect miR-133a-3p level in conditioned medium of BMSCs, while miR-133a-3p level in RNase-A-treated conditioned medium of BMSCs was notably inhibited in the presence of Triton-X-100 (Supplementary Figure 2E). The level of miR-133a-3p was notably upregulated in BMSCs/miR-133a-3p-Exo compared to that in BMSCs-Exo or BMSCs/NC-Exo (Supplementary Figure 2F). Furthermore, miR-133a-3p level in SH-SY5Y cells was significantly upregulated by BMSCs/miR-133a-3p-Exo (Supplementary Figure 2G). To sum up, miR-133a-3p can be transferred from BMSCs to SH-SY5Y cells via exosomes.

Exosomal miR-133a-3p Derived from BMSCs Reversed OGD/R-Induced SH-SY5Y Cell Injury

To detect the function of exosomal miR-133a-3p derived from BMSCs in CI/R injury, SH-SY5Y cells were treated with BMSCs/miR-133a-3p-Exo. As shown in Figure 3A, OGD/R-induced inhibition of miR-133a-3p level in SH-SY5Y cells was significantly reversed by BMSCs/miR-133a-3p-Exo. In addition, BMSCs/miR-133a-3p-Exo notably abolished OGD/R-induced inhibition of SH-SY5Y cell proliferation (Figure 3B and C). Consistently, BMSCs/miR-133a-3p-Exo notably reversed the level of LDH in OGD/R-stimulated SH-SY5Y cells, compared with OGD/R group (Figure 3D). Meanwhile, the pro-apoptotic effect of OGD/R on SH-SY5Y cells was partially reversed by BMSCs/miR-133a-3p-Exo (Figure 3E). Furthermore, OGD/R notably upregulated the level of MDA and inhibited the level of SOD and GSH-Px in SH-SY5Y cells, while that phenomenon was reversed by BMSCs/miR-133a-3p-Exo (Figure 3F–H). In summary, exosomal miR-133a-3p derived from BMSCs reversed OGD/R-induced SH-SY5Y cell injury.

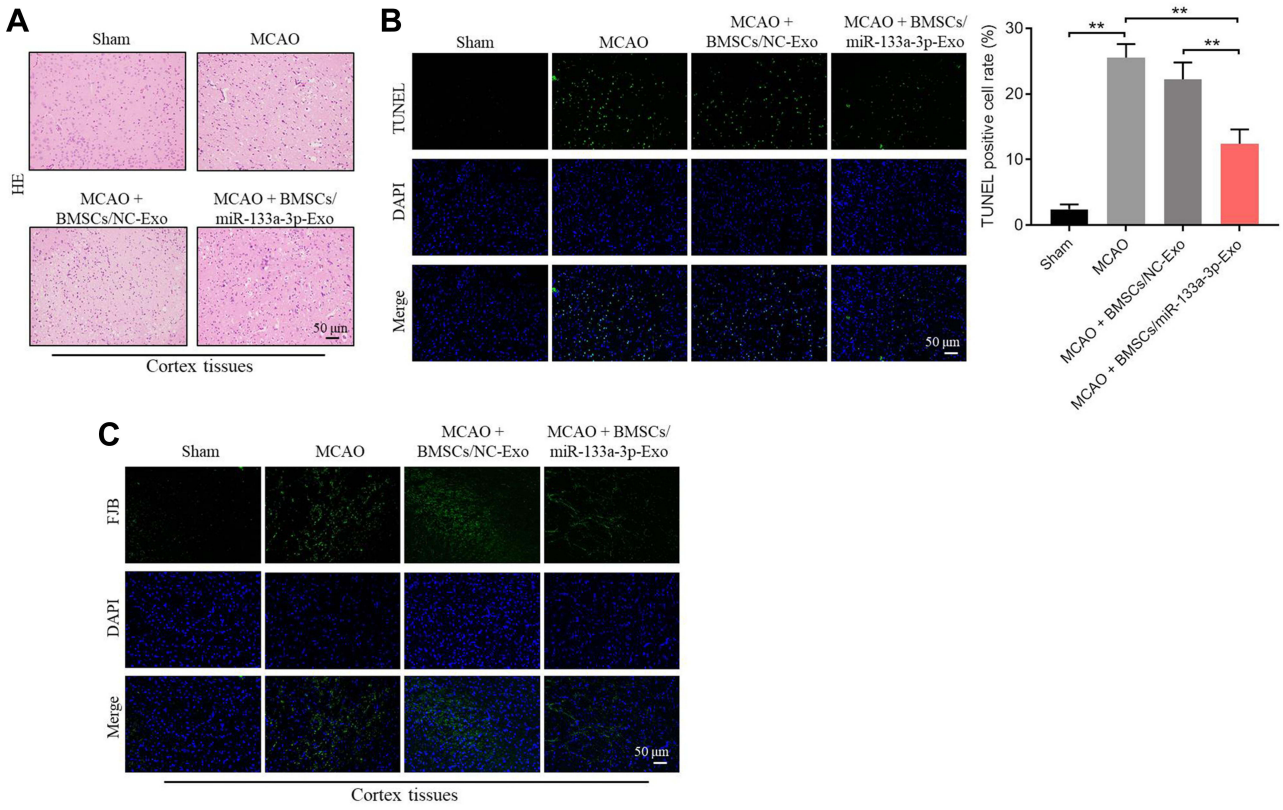

Figure 7 Exosomal miR-133a-3p derived from BMSCs attenuated MCAO-induced hippocampal neuronal degeneration. (**A**) H&E staining was performed to observe the histological changes in brain tissues of rats. (**B**) TUNEL staining was used to investigate the apoptosis in brain tissues of rats. (**C**) FJB staining was used to detect the hippocampal neuronal degeneration. **P< 0.01.

MiR-133a-3p Directly Targeted DAPK2

To explore the target genes of miR-133a-3p, targetscan was used. As shown in Figure 4A, DAPK2 might be a downstream mRNA of miR-133a-3p. Additionally, the luciferase activity in WT-DAPK2 was significantly inhibited by miR-133a-3p mimics (Figure 4B). The level of DAPK2 in SH-SY5Y cells was notably downregulated by upregulation of miR-133a-3p (Figure 4C). Meanwhile, expressions of p-Akt and p-mTOR were significantly reduced, and the expression of DAPK2 was upregulated in OGD/R-treated SH-SY5Y cells (Figure 4D). However, the effect of OGD/R on these proteins was significantly reversed by exosomes with upregulated miR-133a-3p (Figure 4D). Furthermore, DAPK2 level was remarkably higher in plasma of patients with IS than that in healthy people (Figure 4E). DAPK2 overexpression greatly reversed the antiapoptotic effect of exosomal miR-133a-3p on OGD/R-treated SH-SY5Y cells (Figure 4F). To sum up, miR-133a-3p directly targeted DAPK2.

Exosomal miR-133a-3p Derived from BMSCs Alleviated OGD/R-Induced SH-SY5Y Cell Apoptosis via Inhibiting the Autophagy

To explore the relation between exosomal miR-133a-3p and autophagy in CI/R injury, Western blot was used. The expression of Beclin-1 in SH-SY5Y cells was notably upregulated by OGD/R, whereas this phenomenon was partially abolished by exosomes with upregulated miR-133a-3p (Figure 5A). In addition, exosomal miR-133a-3p reversed OGD/R-induced inhibition of cell proliferation via inhibiting the apoptosis, while that effect o was markedly rescued by

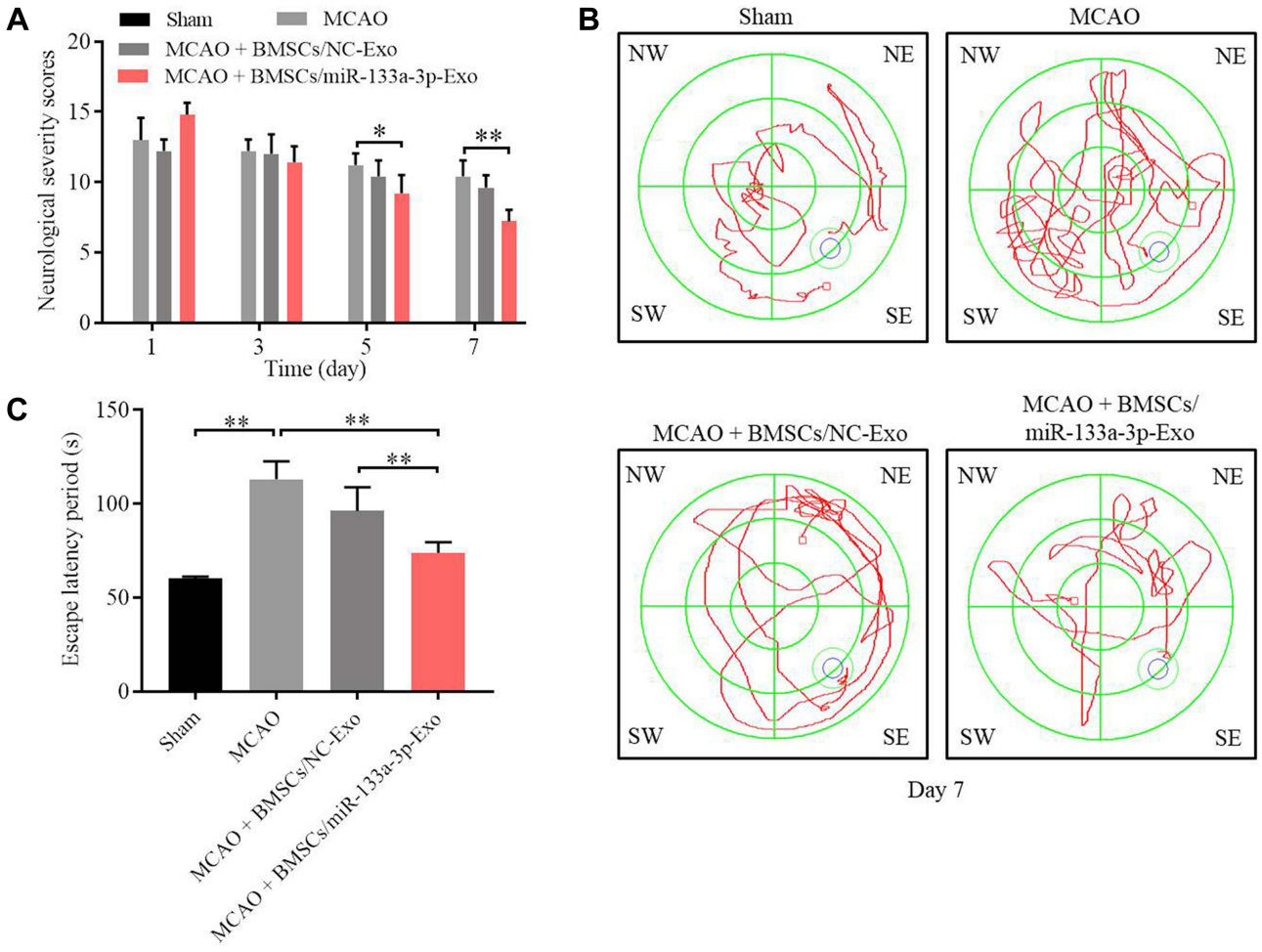

Figure 8 Exosomal miR-133a-3p derived from BMSCs significantly improved the memory capacity of MCAO rats. (**A**) The neurological severity scores of rats were tested. (**B**) Morris Water Maze assay was performed to test the memory capacity of rats. (**C**) The escape latency period of rats were evaluated. *P<0.05, **P< 0.01.

Rapamycin (Figure 5B and C). Thus, it could be suggested that exosomal miR-133a-3p derived from BMSCs alleviated OGD/R-induced SH-SY5Y cell apoptosis via inhibiting the autophagy.

Exosomal miR-133a-3p Derived from BMSCs Markedly Attenuated the Symptom of CI/R Injury in vivo

To further confirm the function of exosomal miR-133a-3p in CI/R injury, in vivo model of CI/R was established. As shown in Figure 6A and B, the cerebral infraction area in rats was obviously upregulated by MCAO surgery, while exosomal miR-133a-3p derived from BMSCs reversed this phenomenon. In addition, MCAO significantly inhibited miR-133a-3p level in tissues of rats, while the effect of MCAO was notably rescued by exosomal miR-133a-3p derived from BMSCs (Figure 6C). Meanwhile, the expressions of p-Akt, p-mTOR was lessened and DAPK2 level was upregulated in MCAO rats, while these changes were reversed by exosomes with upregulated miR-133a-3p (Figure 6D). MCAO notably induced the injury in brain tissues of rats, which was significantly reversed by exosomes with upregulated miR-133a-3p (Figure 7A). Besides, MCAO-induced apoptosis in brain tissues of mice was markedly restored by exosomes containing miR-133a-3p (Figure 7B). Consistently, MCAO induced hippocampal neuronal degeneration in rats, while exosomal miR-133a-3p reversed this phenomenon (Figure 7C). The neurological severity scores (NSS) of rats were notably increased by MCAO surgery, which were reversed by exosomes with upregulated miR-133a-3p (Figure 8A). The results of Morris Water Maze analysis revealed that rats in MCAO + BMSCs/miR-133a-3p-Exo groups exhibited a longer latency time compared with rats in MCAO or MCAO + BMSCs/NC-Exo group (Figure 8B and C). Based on the above data, it could be suggested that exosomal miR-133a-3p derived from BMSCs markedly attenuated the symptom of CI/R injury in vivo.

Discussion

It has been reported that MSCs-derived exosomes could mediate the progression of CI/R via carrying RNAs. MSCs/plasma-derived small extracellular vesicles were able to prevent the CI/R injury[17,18]; Li et al suggested that exosomes with upregulated miR-150-5p derived from BMSCs could mitigate CI/R injury via targeting toll-like receptor 5.[19] Additionally, exosomes derived from CXCR4-overexpressing BMSC could promote activation of microvascular endothelial cells in CI/R Injury.[6] In this research, we found BMSCs-derived exosomes was able to suppress the progression of CI/R injury via carrying miR-133a-3p. Our research firstly explored the role of exosomal miR-133a-3p in CI/R injury, further indicating the mechanism underlying the function of BMSCs-derived exosomes in CI/R injury.

DAPK2 was known to be a key mediator in inflammatory responses.[20] In this research, DAPK2 was identified to be the downstream mRNA of miR-133a-3p. In addition, DAPK2 could negatively regulate Akt signaling.[21,22] Thus, it could be suggested that exosomal miR-133a-3p derived from BMSCs upregulated Akt signaling via targeting DAPK2. Meanwhile, Jiang et al found that DAPK2 could promote the inflammatory responses via activation of NF-κB signaling.[23] Our study was similar to the previous research. NF-κB signaling activation could lead to the inflammatory responses,[24,25] and Akt inactivation could aggravate cell injury.[26] Therefore, the similar function between NF-κB and Akt might contribute to this similarity.

Akt/mTOR signaling is known to be a vital mediator in autophagy.[27,28] In addition, Beclin-1 played a key role in progression of autophagy.[29] Hence, our finding revealed that exosomal miR-133a-3p derived from BMSCs could inhibit the progression of CI/R injury via mediation of Beclin-1 and Akt/mTOR signaling.

Indeed, there are some limitations in this study as follows: 1) some other miRNAs which participated in development of CI/R injury remain unexplored; 2) more targets of miR-133a-3p in CI/R injury are needed to be investigated. Therefore, more analysis are essential in coming future.

In summary, exosomal miR-133a-3p derived from BMSCs alleviates CI/R injury via targeting DAPK2. Thus, our study might supply a theoretical basis for exploring new targets against CI/R injury.

Funding

There is no funding to report.

Disclosure

These authors declared no competing interests in this study.

References

1. Zhu RL, Ouyang C, Ma RL, Wang K. Obstructive sleep apnea is associated with cognitive impairment in minor ischemic stroke. *Sleep Breath*. 2022;26:1907–1914. doi:10.1007/s11325-022-02575-5
2. Lv S, Yang H, Jing P, Song H. alpha-tocopherol pretreatment alleviates cerebral ischemia-reperfusion injury in rats. *CNS Neurosci Ther*. 2022;28:964–970. doi:10.1111/cns.13814
3. Yu G, Sun W, Wang W, et al. Overexpression of microRNA-202-3p in bone marrow mesenchymal stem cells improves cerebral ischemia-reperfusion injury by promoting angiogenesis and inhibiting inflammation. *Aging (Albany NY)*. 2021;13(8):11877–11888. doi:10.18632/aging.202889
4. He H, Zeng Q, Huang G, et al. Bone marrow mesenchymal stem cell transplantation exerts neuroprotective effects following cerebral ischemia/reperfusion injury by inhibiting autophagy via the PI3K/Akt pathway. *Brain Res*. 2019;1707:124–132. doi:10.1016/j.brainres.2018.11.018
5. Zeng Q, Zhou Y, Liang D, et al. Exosomes secreted from bone marrow mesenchymal stem cells attenuate oxygen-glucose deprivation/reoxygenation-induced pyroptosis in PC12 cells by promoting AMPK-dependent autophagic flux. *Front Cell Neurosci*. 2020;14:182. doi:10.3389/fncel.2020.00182
6. Li X, Zhang Y, Wang Y, et al. Exosomes derived from CXCR4-overexpressing BMSC promoted activation of microvascular endothelial cells in cerebral ischemia/reperfusion injury. *Neural Plast*. 2020;2020:8814239. doi:10.1155/2020/8814239
7. Gu J, Wang M, Wang X, et al. Exosomal miR-483-5p in bone marrow mesenchymal stem cells promotes malignant progression of multiple myeloma by targeting TIMP2. *Front Cell Dev Biol*. 2022;10:862524. doi:10.3389/fcell.2022.862524
8. Han L, Liu H, Fu H, et al. Exosome-delivered BMP-2 and polyaspartic acid promotes tendon bone healing in rotator cuff tear via Smad/RUNX2 signaling pathway. *Bioengineered*. 2022;13(1):1459–1475. doi:10.1080/21655979.2021.2019871
9. Qian Y, Chopp M, Chen J. Emerging role of microRNAs in ischemic stroke with comorbidities. *Exp Neurol*. 2020;331:113382. doi:10.1016/j.expneurol.2020.113382
10. Shi Y, Yi Z, Zhao P, Xu Y, Pan P. MicroRNA-532-5p protects against cerebral ischemia-reperfusion injury by directly targeting CXCL1. *Aging*. 2021;13(8):11528–11541. doi:10.18632/aging.202846
11. Zuo ML, Wang AP, Song GL, Yang ZB. miR-652 protects rats from cerebral ischemia/reperfusion oxidative stress injury by directly targeting NOX2. *Biomed Pharmacother*. 2020;124:109860. doi:10.1016/j.biopha.2020.109860
12. Zhang Y, Tu B, Sha Q, Qian J. Bone marrow mesenchymal stem cells-derived exosomes suppress miRNA-5189-3p to increase fibroblast-like synoviocyte apoptosis via the BATF2/JAK2/STAT3 signaling pathway. *Bioengineered*. 2022;13(3):6767–6780. doi:10.1080/21655979.2022.2045844
13. Wu R, Soland M, Liu G, et al. Functional characterization of the immunomodulatory properties of human urine-derived stem cells. *Transl Androl Urol*. 2021;10(9):3566–3578. doi:10.21037/tau-21-506
14. Lu Y, Gao H, Zhang M, Chen B, Yang H. Glial cell line-derived neurotrophic factor-transfected placenta-derived versus bone marrow-derived mesenchymal cells for treating spinal cord injury. *Med Sci Monit*. 2017;23:1800–1811. doi:10.12659/MSM.902754
15. Liu Y, Zhu X, Tong X, Tan Z. Syringin protects against cerebral ischemia/reperfusion injury via inhibiting neuroinflammation and TLR4 signaling. *Perfusion*. 2021;37:562–569.
16. Li Z, Li A, Yan L, et al. Downregulation of long noncoding RNA DLEU1 attenuates hypersensitivity in chronic constriction injury-induced neuropathic pain in rats by targeting miR-133a-3p/SRPK1 axis. *Mol Med*. 2020;26(1):104. doi:10.1186/s10020-020-00235-6
17. Dumbrava DA, Surugiu R, Borger V, et al. Mesenchymal stromal cell-derived small extracellular vesicles promote neurological recovery and brain remodeling after distal middle cerebral artery occlusion in aged rats. *Geroscience*. 2022;44(1):293–310. doi:10.1007/s11357-021-00483-2
18. Driga MP, Catalin B, Olaru DG, et al. The need for new biomarkers to assist with stroke prevention and prediction of post-stroke therapy based on plasma-derived extracellular vesicles. *Biomedicines*. 2021;9:9. doi:10.3390/biomedicines9091226
19. Li X, Bi T, Yang S. Exosomal microRNA-150-5p from bone marrow mesenchymal stromal cells mitigates cerebral ischemia/reperfusion injury via targeting toll-like receptor 5. *Bioengineered*. 2022;13(2):3030–3043. doi:10.1080/21655979.2021.2012402
20. Liu H, Zhang L, Li M, et al. Bone mesenchymal stem cell-derived extracellular vesicles inhibit DAPK1-mediated inflammation by delivering miR-191 to macrophages. *Biochem Biophys Res Commun*. 2022;598:32–39. doi:10.1016/j.bbrc.2022.02.009
21. Szoltysek K, Ciardullo C, Zhou P, et al. DAP kinase-related apoptosis-inducing protein kinase 2 (DRAK2) is a key regulator and molecular marker in chronic lymphocytic leukemia. *Int J Mol Sci*. 2020;21:20. doi:10.3390/ijms21207663
22. Wu YH, Chou TF, Young L, et al. Tumor suppressor death-associated protein kinase 1 inhibits necroptosis by p38 MAPK activation. *Cell Death Dis*. 2020;11(5):305. doi:10.1038/s41419-020-2534-9
23. Jiang Y, Liu J, Xu H, et al. DAPK2 activates NF-kappaB through autophagy-dependent degradation of I-kappaBalpha during thyroid cancer development and progression. *Ann Transl Med*. 2021;9(13):1083. doi:10.21037/atm-21-2062
24. Xuan L, Fu D, Zhen D, et al. Long non-coding RNA Sox2OT promotes coronary microembolization-induced myocardial injury by mediating pyroptosis. *ESC Heart Fail*. 2022;9:1689–1702. doi:10.1002/ehf2.13814
25. Li O, Zhao C, Zhang J, et al. UBAP2L promotes gastric cancer metastasis by activating NF-kappaB through PI3K/AKT pathway. *Cell Death Discov*. 2022;8(1):123. doi:10.1038/s41420-022-00916-7
26. Huang Y, Wang Y, Wu Z, et al. SOX11-dependent CATSPER1 expression controls colon cancer cell growth through regulation the PI3K/AKT signaling pathway. *Genes Genomics*. 2022;44(11):1415–1424. doi:10.1007/s13258-022-01240-1
27. Gawande DY, Kumar SNK, Bhatt JM, et al. Glutamate delta 1 receptor regulates autophagy mechanisms and affects excitatory synapse maturation in the somatosensory cortex. *Pharmacol Res*. 2022;178:106144. doi:10.1016/j.phrs.2022.106144
28. Tang ZL, Zhang K, Lv SC, et al. Corrigendum to "LncRNA MEG3 suppresses PI3K/AKT/mTOR signalling pathway to enhance autophagy and inhibit inflammation in TNF-alpha-treated keratinocytes and psoriatic mice" [Cytokine 148 (2021) 155657]. *Cytokine*. 2022;153:155853. doi:10.1016/j.cyto.2022.155853
29. Shao W, Wang S, Wang X, et al. miRNA-29a inhibits atherosclerotic plaque formation by mediating macrophage autophagy via PI3K/AKT/mTOR pathway. *Aging*. 2022;14(5):2418–2431. doi:10.18632/aging.203951